Presence of Heterogeneities in Rocks during Laboratory Waterfloods: A Case Study Highlighting Differences in Relative Permeabilities between Homogeneous and Heterogeneous 1D Approaches

Fabrice Pairoys[1,*], *Vitaliy* Afanasiev[2], *Roland* Lenormand[3], *Guillaume* Lenormand[3], *Cyril* Caubit[4]

[1]SLB, Tornado tower, 45th floor, Doha, Qatar
[2]SLB Reservoir Laboratories, 6350 West Sam Houston Parkway North, Houston, United States
[3]Cydarex, 130 rue du port, 44420 Mesquer, France
[4]TotalEnergies, CSTJF, Avenue Larribau, 64018 Pau Cedex, France

Abstract.
In Special Core Analysis, relative permeabilities Kr are obtained from laboratory coreflooding tests using unsteady-state, steady-state, or semi-dynamic methods. To better represent the reservoir conditions, these tests are performed at the reservoir conditions with live fluids. While restoring a representative wettability state is crucial, a significant challenge remains in accurately selecting representative rock samples.
It is always preferred to perform the coreflooding tests on homogeneous samples. For selecting the most homogeneous rock samples, several methods are used: CT imaging, minipermeametry, miscible tracer tests, x-ray attenuation technique (porosity distribution and saturation profiles), nonlinear differential pressure before breakthrough during primary drainage.
When dealing with carbonate rocks, selecting homogeneous samples becomes a challenge: it is sometimes impossible to find a homogeneous rock without small-scale heterogeneity features. Moreover, some companies even prefer selecting samples containing small-scale heterogeneities (along or/and across core axis heterogeneities), because they are a true representation of their reservoir quality, with respect to directional injection scenario.
Pairoys *et al.* published a paper at the 2024 Society of Core Analysts symposium discussing different methods to account for rock heterogeneity when interpreting the waterflooding lab results. Using the heterogeneous approach called the Egermann method, they successfully history-matched the noisy saturation profiles obtained during a steady-state waterflooding test performed on a heterogeneous rock. It was also shown that there were no significant Kr differences between the classical homogeneous method and the Egermann method. It raised the question of the need to use the Egermann method, just for the sake of a better history-match quality. In the case study presented in this paper, we demonstrate that differences in Kr curves can be observed: not using the Egermann method when interpreting waterflooding tests on heterogeneous rocks may lead to overly optimistic Kr curves.

1 Introduction

When measuring relative permeabilities at the laboratory, the selection of the most homogeneous rock samples is a crucial step: at this condition, the coreflooding experiments are reliable way to estimate the microscopic efficiency. When dealing with heterogeneous rocks, microscopic and sweep efficiency are combined. The quest of homogeneous samples becomes particularly challenging with carbonate rocks. Pairoys *et al.* [1] listed the conventional methods used to select the most homogeneous samples before performing a SCAL program: CT imaging, minipermeametry, mercury injection capillary pressure MICP and tracer test technique. During the tests, x-ray porosity and irreducible water saturation Swi profiles, and/or nonlinear differential pressure before breakthrough during primary drainage also help in assessing the degree of heterogeneity of the rocks. Pairoys *et al.* [1] also refers to a bibliography about the effect of small-scale heterogeneity on relative permeability. The takeaway message is that, ignoring small-scale heterogeneity may generate large errors in the determination of relative permeabilities. In general, if the rock sample is heterogeneous, small-scale heterogeneity must be captured by experimental measurements and considered in the Kr interpretation (numerical simulations). We recommend reading this paper where some important references can be found.

In this new study, a similar workflow described in Pairoys *et al.* [1] was used: this workflow is based on the method described by Lombard *et al.* [2] and Egermann *et al.* [3]. For simplification, the method will be called Egermann method in the following sections: it assumes that local

* Corresponding author: fpairoys@slb.com

variations of pressure field in heterogeneous medium are much smaller than saturation variations. It is based on upscaling techniques routinely applied in reservoir simulation, considering that the pressure is a long-range field that averages the local fluctuations. Consequently, local capillary pressure Pc curves can be obtained from the simulated pressure profiles after performing a numerical interpretation considering homogeneous porous medium, we will call it homogeneous approach.

Pairoys *et al.* [1] tested different approaches to derive the permeability profile from the x-ray porosity profile. Based on their results, the constant permeability and Kozeny-Carman permeability profiles with local capillary pressures were tested in this new study. The constant permeability method is not presented in this paper because it was not able to history-match the saturation profiles as well as the Kozeny-Carman model. Only the results from Egermann method combined with Kozeny-Carman permeability profile are presented.

The commercial software CYDAR was used to perform numerical simulations and optimizations via automatic history-matching process. It allows to input non-uniform initial saturation profile, porosity and permeability profiles and multiple capillary pressures along the sample, but with a unique set of relative permeabilities.

Like in Pairoys *et al.* [1], it is shown that the heterogeneous approach improves the history-match quality of the experimental data (oil production and differential pressure) while reproducing the noisy saturation profiles with good accuracy. This point is an improvement for the quality control of the simulation. But unlike in Pairoys *et al.* [1], the relative permeabilities determined with the heterogeneous simulations are found to be different to those determined by considering the rock homogeneous.

2 Experimental Description

2.1 Rock and fluid properties

A heterogeneous carbonate rock was selected for this case study. CT images have shown presence of cross-bedding heterogeneity with varying matrix density and presence of vugs along the sample, as shown in Figure 1.

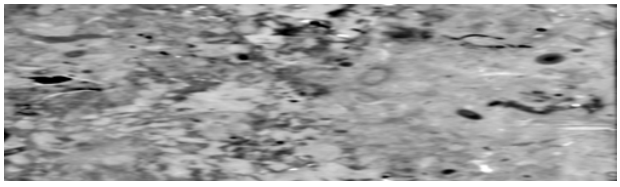

Fig. 1. CT image from the rock.

The heterogeneous characteristic of this rock was also confirmed by a brine/brine miscible tracer test (MTT) in Figure 2, highlighting an early concentration breakthrough of the injected brine and long production tail to reach concentration equilibrium.

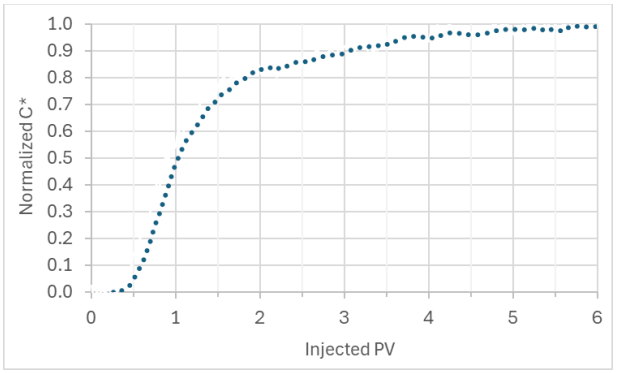

Fig. 2. Elution curve from MTT.

MICP tests were performed on three samples taken at close depth of the core; it is observed that the pore throat size distribution varies from one sample to another, pore throat radius varying from 0.01 micron to 20 microns: according to the location where the sample is taken, large differences in pore throat size distribution (PTSD) can be observed, as shown in Figure 3.

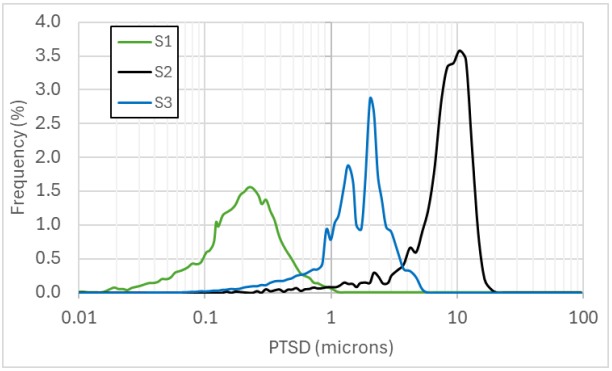

Fig. 3. MICP pore throat size distribution (PTSD) of 3 samples.

All the above observations highlight the presence of small-scale heterogeneities along/across the sample. It can be concluded that this core is a good candidate for studying the effect of small-scale heterogeneities on relative permeabilities.

The rock dimensions, average porosity and brine permeability are provided in Table 1.

Table 1. Rock properties.

Length (cm)	Diameter (cm)	Porosity φ (%)	Permeability Kw (mD)
12.81	3.80	25.02	2.78

The single long core pore volume (PV=36.29 cc) reduces the uncertainty on the average saturation calculated by material balance. Using a single long core sample also reduces the risk of capillary contact loss when using composite stack.

The brine and live oil properties, at reservoir conditions, are listed in Table 2.

Table 2. Fluid properties.

	Density ρ (g/cc)	Viscosity μ (cP)
Brine	1.05	0.41
Live oil	0.80	0.78

Brine and live oil have been equilibrated to avoid any mass transfer during the waterflooding test. The steady-state experiment was performed at reservoir conditions (temperature of 95°C, pore pressure of 110 bar, net confining pressure of 140 bar).

Note that, after saturating the rock with doped formation brine, x-ray attenuation technique was used to determine the porosity profile: acquisition of the porosity profile is of importance for testing the proposed workflow.

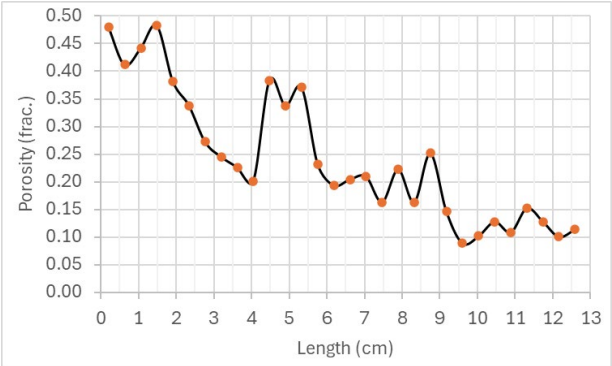

Fig. 4. Porosity φ profile.

Figure 4 confirms the heterogeneous character of the selected rock, with porosity spatially varying from 9% to 48%. Because there was no local permeability K measurement, Kozeny-Carman method, [4] [5], has been used to derive the permeability profile (described later).

When dealing with heterogeneous samples, it is recommended to use the steady-state method to limit the detrimental effect of small-scale heterogeneity during waterflooding tests. Then, it is also recommended using numerical simulation means to derive relative permeabilities, as laboratory coreflooding tests may be affected by end-effects, even during steady-state tests.

2.2 Experimental protocol

An imbibition steady-state experiment was performed at immiscible reservoir conditions, with the sample vertically oriented and fluids injected from bottom to top.

A closed-loop steady-state coreflooding system was used in this study. It included high-range pressure and differential pressure transducers to record the evolution of the inlet-outlet differential pressure over time, a high-pressure high-temperature visual separator to monitor the fluid volume balance or material balance (MB), and a 1D linear x-ray scanner to monitor the saturation profiles at 30 different locations. These locations correspond to 30 points where local porosity and local saturation are measured.

The rock was brought to the irreducible water saturation Swi of 24.9% using viscous displacement method: the Swi target was obtained from porous plate capillary pressure Pc tests, used for saturation modeling in the study. Because of the presence of capillary end-effect, reverse injection was performed to ensure the most representative saturation and wettability distributions as possible. The viscous mineral oil was then replaced by dead oil (with intermediate decalin flushing to avoid asphaltenes precipitation) for a dynamic ageing at reservoir temperature for 4 weeks. Finally, the dead oil was replaced with live oil. The imbibition cycle was then performed with live brine (equilibrium between live oil and brine to avoid exchanges between phases). A new scan is made to visualize the saturation profile at Swi (Figure 5).

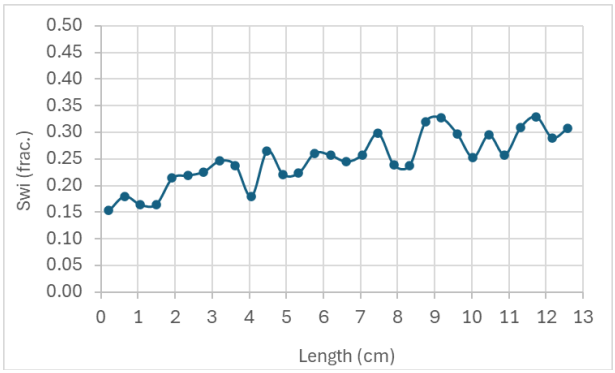

Fig. 5. Irreducible water saturation Swi profile after ageing.

It can be noted that, despite all precautions taken to flatten the Swi saturation profile (average Swi of 24.9%), significant local variations of saturation are observed, mainly due to the degree of heterogeneity of the rock. Even if the overall trend of the Swi profile tends to follow the observed porosity profile trend (decrease in porosity from left to right leads to an increase in Swi from left to right), it is difficult to correlate local Swi to the local porosity values. Local Swi values vary from 15.2% to 32.9%.

For the steady-state method, 6 rate ratios and 1 bump rate were planned after a preliminary design step using Cydar software. The resulting ratios/bump rates that have been applied during the waterflooding are listed in Table 3.

Table 3. Water-oil rates for SS test.

	Qw (cc/min)	Qo (cc/min)	Qw/Qt ratio (%)
1	0.125	1.875	6.25
2	0.560	1.440	28.00
3	1.387	0.613	69.35
4	1.861	0.139	93.05
5	1.975	0.025	98.75
6	2.000	0.000	100.00
7	4.000	0.000	100.00

3 Experimental Results

As said earlier, the steady-state test is performed at a total constant rate, monitoring oil volume balance, differential pressure and saturation profile along the rock sample.

Figures 6 and 7 represent the produced oil and differential pressure versus time during the two-phase flow steady-state test.

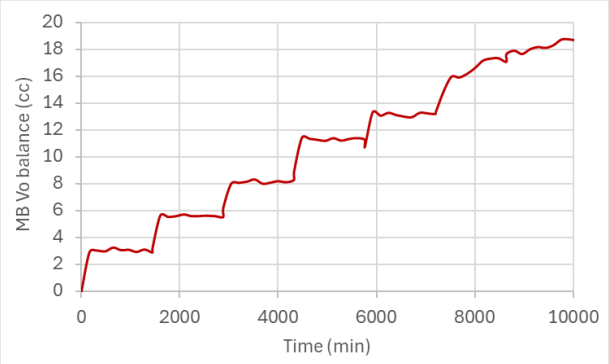

Fig. 6. Experimental oil volume balance versus time.

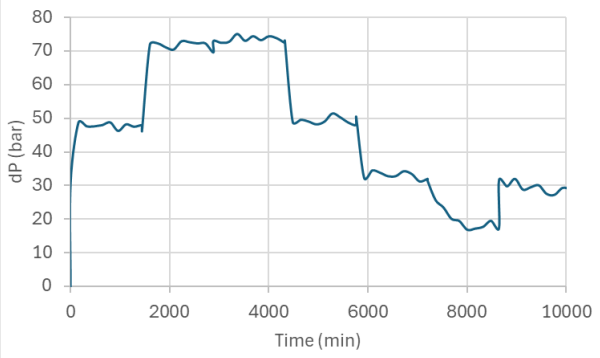

Fig. 7. Experimental differential pressure versus time.

The equilibrium of the oil volume balance (produced oil from the sample) and differential pressure was obtained at the end of each ratio.

Saturation profiles were also used to confirm that an acceptable equilibrium was reached before changing the rate ratios. The saturation profiles at the end of each ratio and each bump rate are presented in Figure 8. At end of each step, average saturation from x-ray technique and dP are taken to determine the analytical relative permeabilities, assuming uniform saturation and no capillary pressure.

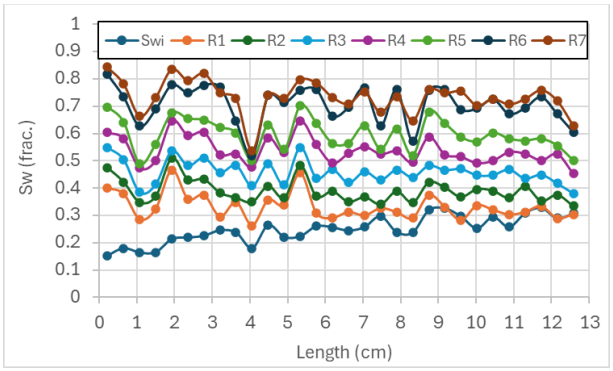

Fig. 8. Experimental saturation profiles.

As for porosity and Swi profiles, large spatial fluctuations of saturation at equilibrium are observed. All can guess that using a homogeneous approach to interpret experimental data cannot history-match the saturation profiles.

As a QC step, derived average water saturation from x-ray attenuation technique was compared to the material balance (MB) water saturation using the visual separator:

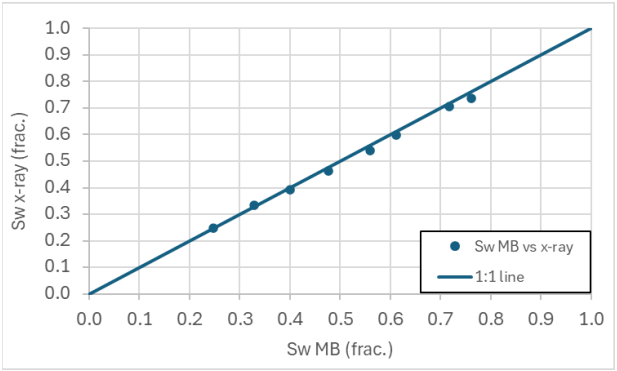

Fig. 9. Comparison between x-ray and material balance water saturation values.

Figure 9 shows good agreement between the two different methods. Average water saturation from x-ray attenuation technique was chosen for computing the Kr curves.

4 "Homogeneous" Interpretation

The homogeneous approach consisted in plotting the analytical SS Kr data points, fitting them with a Corey model, performing a preliminary history-match of the data with no capillary pressure. Then a logBeta function was used to model the capillary pressure Pc.

Equations 1, 2 and 3 represent the Corey equations used to model Kr in this study:

$$k_{rw} = K_{rw}\ Max.(S_w^*)^{Nw} \quad (1)$$

$$k_{ro} = k_{ro}\ Max.(1 - S_w^*)^{No} \quad (2)$$

$$S_w^* = \frac{S_w - S_{wi}}{1 - S_{wi} - S_{or}} \quad (3)$$

With Krw and Kro the relative permeabilities of water and oil respectively, Sw* the reduced saturation, Nw and No the Corey exponents of water and oil respectively, Sw the

varying water saturation, Swi the irreducible water saturation, Sor the residual oil saturation. The Krw Max value corresponds to the water relative permeability at the end of the waterflooding test and Kro Max corresponds to the oil relative permeability at the beginning of the test (equal to 1 here as the effective oil permeability at Swi is taken as reference permeability to calculate Kr).

The logBeta equation, similar to the equation described in [6], is used to model the capillary pressure Pc (Equation 4):

$$Pc = cP_o \ ln\frac{(1-Sw^{*\beta})}{Sw^{*\beta}} - b \qquad (4)$$

With Po a pressure coefficient to control the magnitude of the Pc curve, Sw* the reduced saturation, β coefficient to control the asymmetry of the function, b a function dependent on the water saturation at Pc=0, and c parameter calculated as a function of β to impose a slope equal to Po at the middle of the Pc curve (Sw*=0.5). In the simulator, only Po, β and Sw at Pc=0 are tuned (due to some dependency of parameters from Equation 4).

The history-match process is done again by tuning both Kr and Pc parameters. The resulting Kr and Pc curves are presented below (Figure 10, Figure 11, and Figure 12).

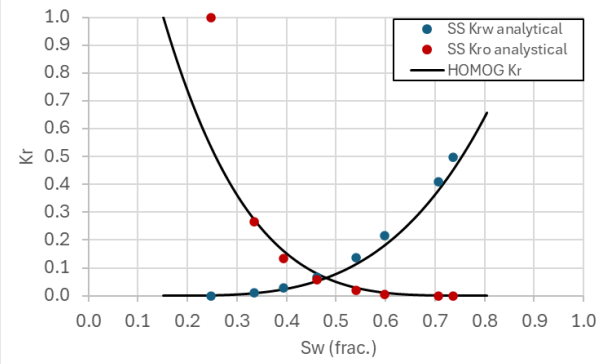

Fig. 10. Analytical steady-state data points and post-interpreted Kr using homogeneous approach (cartesian plot).

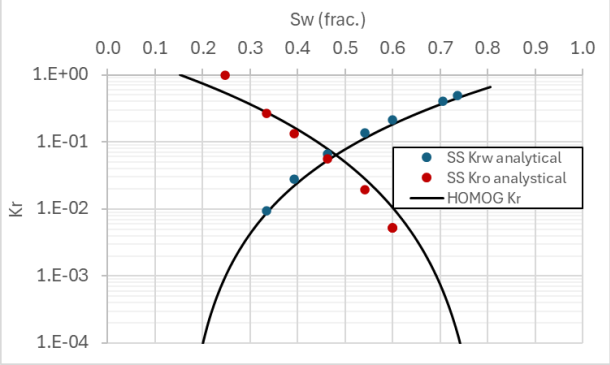

Fig. 11. Analytical steady-state data points and post-interpreted Kr using homogeneous approach (semi-log plot).

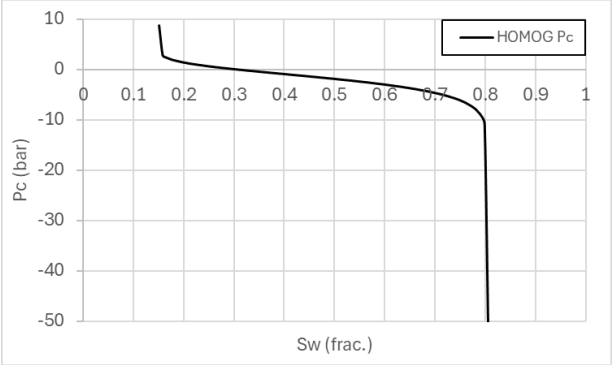

Fig. 12. Post-interpreted Pc.

The resulting parameters (Corey model and logBeta function) are listed in Table 4.

Table 4. Kr and Pc parameters (KroMax=1 and Swi=0.152, Po in bar).

Nw	No	KrwMax	Sor	Po	β	Sw@Pc=0
3.40	3.94	0.66	0.195	6.4	0.1	0.300

Note that Swi value for the interpretation was taken equal to 0.152 and not to the average Swi of 0.249: it allows to history-match the Swi profile, where local saturations can go down to 0.152.

The resulting water fractional flow Fw and Kr ratio are presented in Figure 13 and Figure 14.

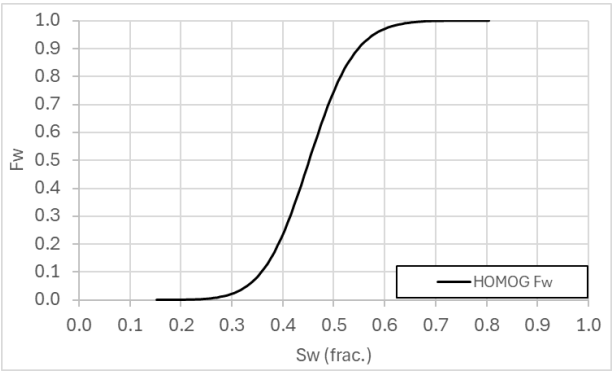

Fig. 13. Post-interpreted fractional flow Fw.

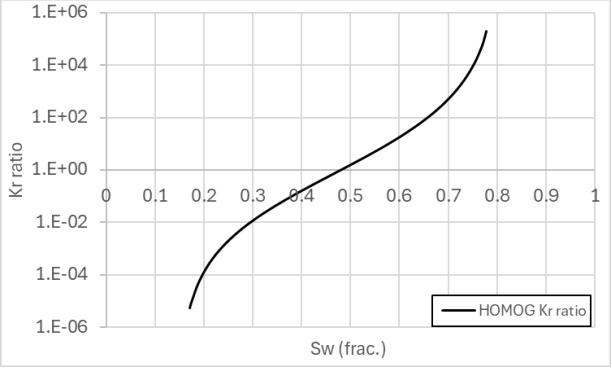

Fig. 14. Post-interpreted Kr ratio.

The history-match quality using homogeneous approach is shown in Figure 14, Figure 15, and Figure 16.

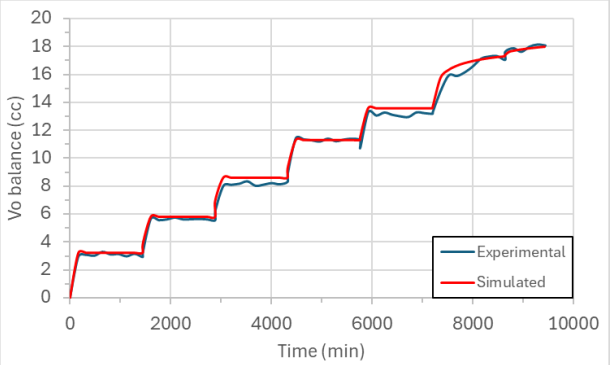

Fig. 15. Experimental versus simulated oil volume balance.

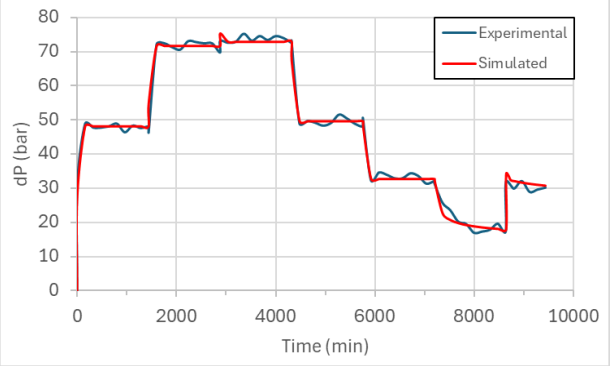

Fig. 16. Experimental versus simulated dP history-match.

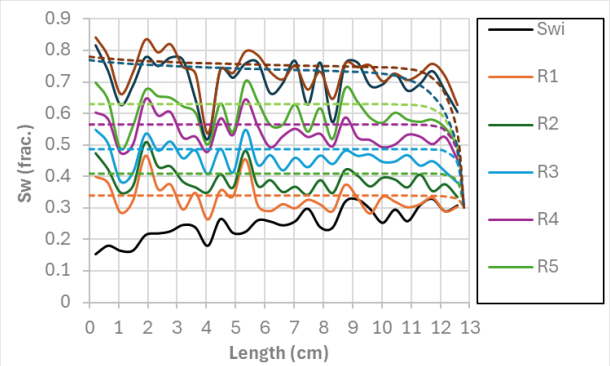

Fig. 17. Experimental (plain lines) versus simulated (dashed lines) saturation profiles.

If the history-match quality of the oil volume balance and dP signals (Figure 15 and Figure 16 respectively) is acceptable, it is, as expected, not possible to history-match the experimental saturation profiles (Figure 17) using the homogeneous approach. Note that, in our optimization process, we have used higher weight to history-match the oil production, slightly degrading the history-match of the dP signal. Same weight has been used for all optimizations, including those using heterogeneous approaches, to keep good consistency in our interpretations.

5 "Heterogeneous" Interpretation

To start with the heterogeneous approach listed earlier in the introduction section, 30 Pc curves using Egermann method were extracted from the homogeneous approach.

In addition to the saturation profiles at equilibrium, water and oil pressure profiles (respectively Figure 18 and Figure 19) from the homogeneous simulation were taken to reconstruct the local Pc curves: at each x-ray point (30 points) corresponds 1 Pc, built by simply subtracting local simulated water pressure to the local simulated oil pressure (Pc=Po-Pw) at equilibrium and taking the respective water saturation at the end of each ratio.

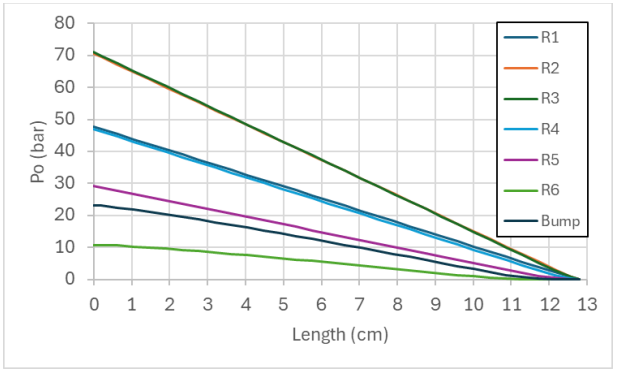

Fig. 18. Simulated oil pressure profiles obtained from "homogeneous" approach.

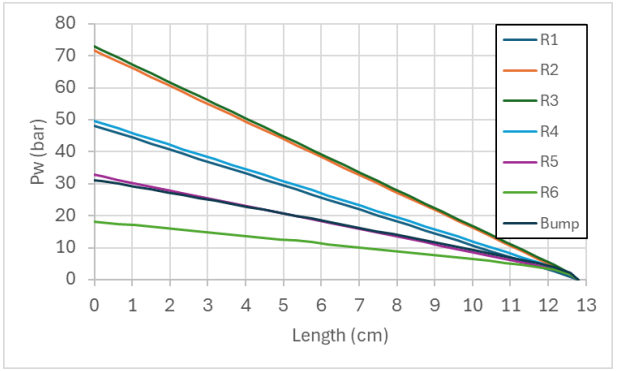

Fig. 19. Simulated water pressure profiles obtained from "homogeneous" approach.

Using local pressures and saturations, the 30 Pc curves can be built (Figure 20).

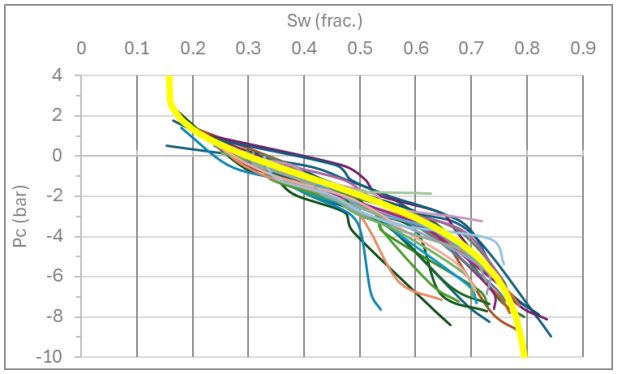

Fig. 20. Thirty local Pc and Pc from homogeneous interpretation in yellow.

The variability of the Pc curves results from the degree of heterogeneity of the rock. They are still found in the same range as the single Pc curve from the homogeneous approach in yellow. For the management of uncertainties,

the envelop of local Pc curves is very useful information for reservoir simulations.

The next step was to build the heterogeneous medium in the simulator. Thirty blocks of varying properties (porosity, permeability and capillary pressure) were placed in parallel as shown in Figure 21.

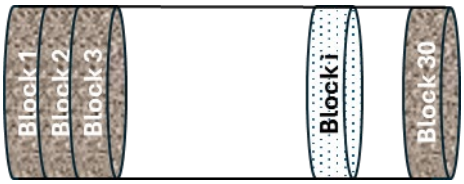

Fig. 21. 30 blocks of varying porosity, permeability and capillary pressure.

In their 2024 study, Pairoys *et al.* [1] concluded that the Egermann method was the best approach for history-matching the noisy saturation profiles, and the Leverett approach failed to reproduce the amplitude of the measured saturation profiles. It was decided to interpret our results with the Egermann method.

Then, in the same 2024 paper, Pairoys *et al.* made several attempts of history-match using constant local permeability profile, Kozeny-Carman profile and Timur profile [7]. It was observed that using constant permeability profile led to best history-match quality: the given explanation was that local permeability fluctuations are averaged due to the long-range correlation of the pressure field and do not contribute to saturation fluctuations. In the present study, constant permeability profile and Kozeny-Carman permeability profile were tested: it turned out that, in addition to the Egermann method, the Kozeny-Carman permeability profile gave the best result, questioning the previous statement. Only the results from the Egermann method with permeability profile from Kozeny-Carman model are presented and compared to the homogeneous and classical approach. In the following, a simplified Kozeny-Carman model (Eq. 5) was used to input local permeability at each block:

$$K_{i(K-C)} = \frac{\varphi_i^3 d_p^2}{180(1-\varphi)^2} \qquad (5)$$

With $K_{i(K\text{-}C)}$ the Kozeny-Carman local permeability, φ_i the local porosity and dp the average grain diameter (3.8 µm) calculated using the Kozeny-Carman equation with the average porosity and permeability values from Table 1.

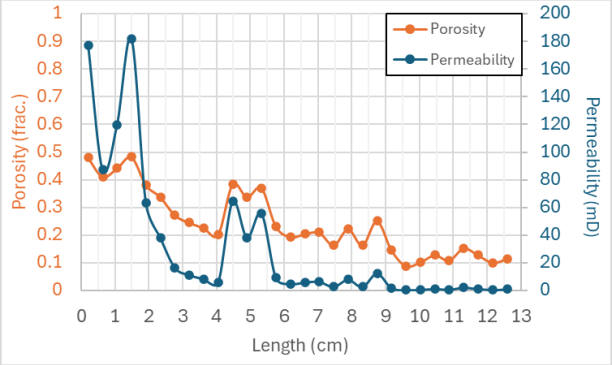

Fig. 22. Local porosity (orange) and Kozeny-Carman permeability distribution (blue).

Note that the harmonic average of the 30 permeability values was normalized to be equal to the average rock permeability from Table 1.

History-match quality of oil volume balance and dP signals, obtained with the core analysis simulator, are shown in Figure 23 and Figure 24.

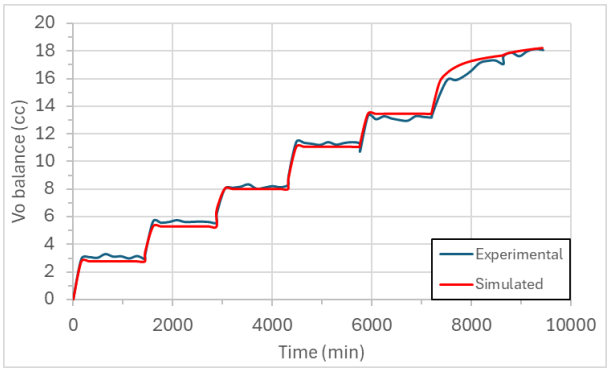

Fig. 23. History-match result of the oil volume balance.

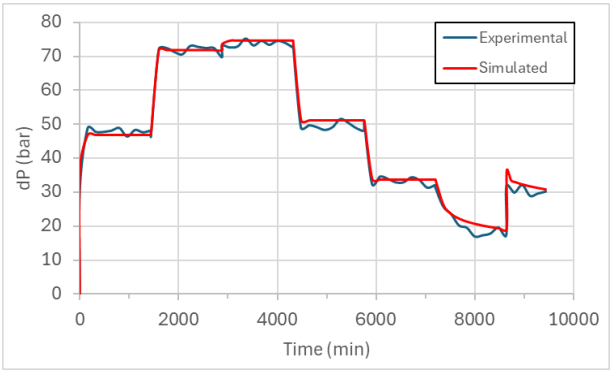

Fig. 24. History-match result of the dP signal.

An acceptable history-match quality was obtained. When comparing with Figures 15 and 16, similar history-match quality is found between the homogeneous and heterogeneous methods.

History-match of the saturation profiles using the heterogeneous approach is shown in Figure 25.

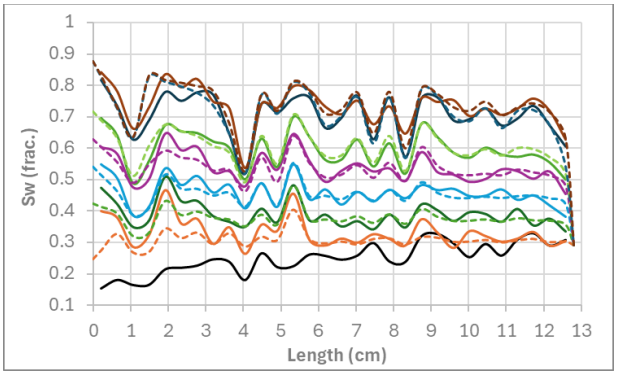

Fig. 25. Experimental (dashed lines) versus simulated (plain lines) saturation profiles using heterogeneous approach 1.

The simulated saturation profiles (dashed lines) reproduce well the saturation variations observed on the experimental profiles (plain lines), with a good representation of the local saturation amplitudes.

Note that there was no need to make an additional iteration, as suggested by Egermann: the simulated saturation profiles and overall history-match quality were found to be good enough.

6 Comparison between Homogeneous and Heterogeneous Results

In the previous section, it was shown that the history-match quality was improved when using the heterogeneous approach. It confirms the observations made by Pairoys *et al.* [1]. In their paper, they also notice that there were no significant differences between the resulting Kr curves, whatever the tested homogeneous or heterogeneous approaches: the only observed difference between the homogeneous method, Leverett method and Egermann method was a decrease in Sor when using the last method (Figure 26).

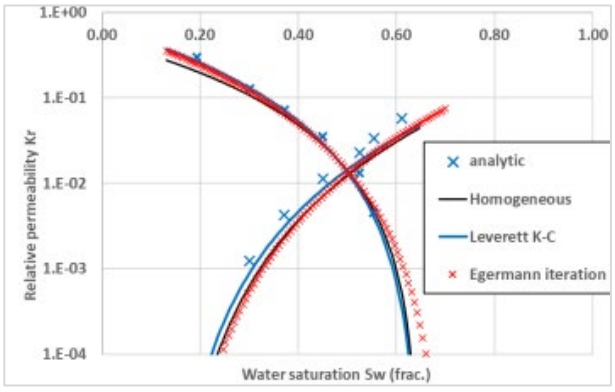

Fig. 26. Comparison between the Kr curves using different methods, extracted from the 2024 reference [1].

The comparison is now conducted using the new dataset from the recent study. The Kr curves are analyzed to determine whether the observations highlighted by Pairoys *et al.* [1] are corroborated. Figures 27 to 30 present the Cartesian and semi-log Kr, Kr ratio, and Fw curves.

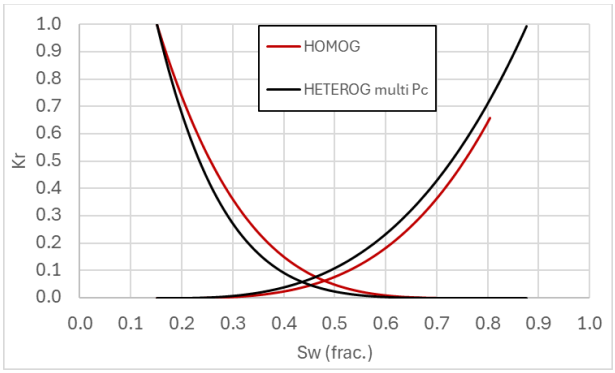

Fig. 27. Cartesian Kr curves comparison.

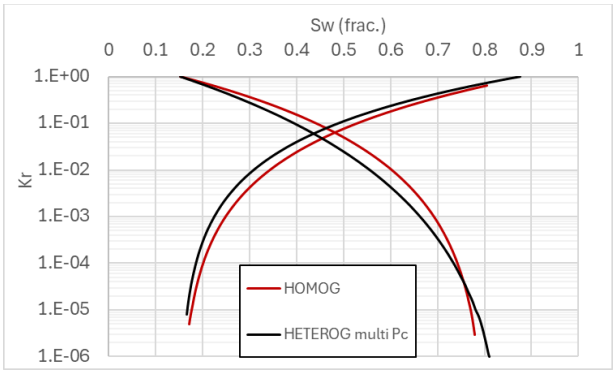

Fig. 28. Semi-log Kr curves comparison.

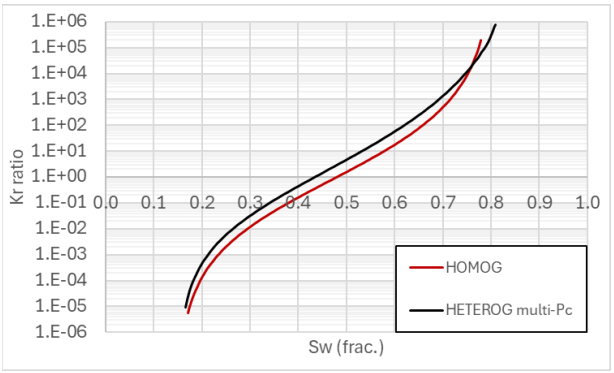

Fig. 29. Kr ratio curves comparison.

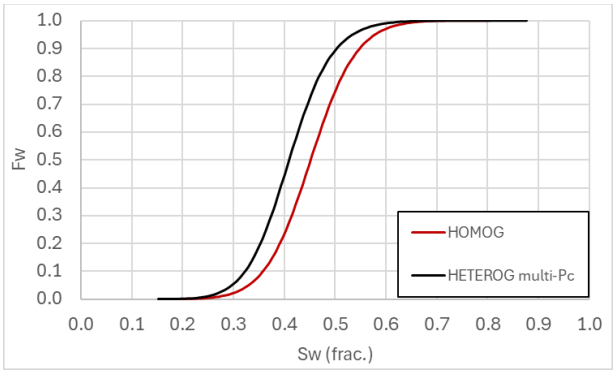

Fig. 30. Fw curves comparison.

The coefficients of the Kr Corey model, using the homogeneous and heterogeneous approaches, are shown in Table 5.

Table 5. Kr parameters (Swi=0.152 & KroMax=1).

	Nw	No	KrwMax	Sor
HOMOG	3.40	3.94	0.66	0.195
HETEROG	3.01	5.65	0.99	0.124

If the heterogeneous approach helps in better history-matching the experimental data, especially the saturation profiles, it also leads to different resulting Kr parameters. If the Kr and Kr ratio curves look quite similar, the fractional flow curve highlights a difference: Figure 30 shows that Fw curve from the heterogeneous approach is less optimistic than that from the homogeneous one.

To assess the difference between the two approaches, a Buckley-Leverett analysis was performed to highlight the differences in original oil in place (OOIP) recovery factor.

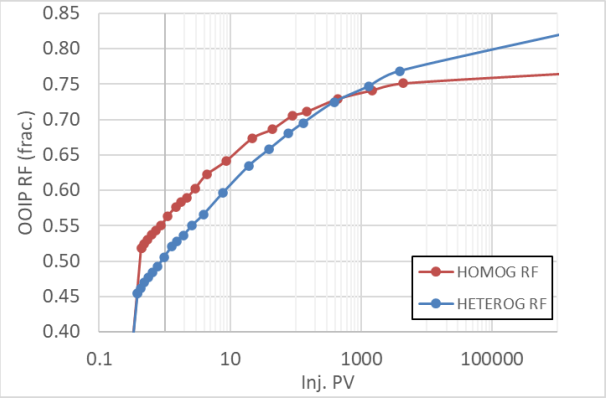

Fig. 31. Oil recovery factor RF versus injected PV based on Buckley-Leverett analysis.

Figure 31 highlights two different recovery trends according to the interpretation. Table 6 summarizes the oil recovery according to the number of injected PVs.

Table 6. OOIP recovery factors.

	HOMOG	HETEROG
Inj. PV @ BT	0.44	0.39
OOIP RF @ BT	0.52	0.45
OOIP RF @ 1PV	0.56	0.51
OOIP RF @ 10PV	0.65	0.61
OOIP RF @ 10^5PV	0.76	0.80

Table 6 indicates that the homogeneous approach results in the most optimistic recovery factor, characterized by a delayed breakthrough and higher recovery factor RF up to 400 pore volumes PVs of injected fluid. Beyond 400 PVs, the RF achieved using the heterogeneous approach surpasses that of the homogeneous approach.

Combining fractional flow, Kr parameters and Buckley-Leverett analysis, it is shown that that the heterogeneous approach results in a more oil-wet-like behavior. Using the homogeneous Kr at the reservoir scale will lead to a more optimistic scenario.

7 Discussion

The selected rock had a large degree of heterogeneity, with possible combined across bedding flow and presence of vugs (highlighted on the CT image in Figure 1), but also along-bedding flow (highlighted by the MTT in Figure 2). MICP data results (Figure 3) also showed that PTSD may vary a lot at the centimetric scale. The problem is how to account for the heterogeneity in the simulation. From x-ray measurements, we obtain the porosity and saturation profiles. It is important to note that these profiles are determined along the x-ray beam with a few mm diameter and may differ from the average values across the sample that are used for numerical saturation. A 2D or 3D approach would help in capturing all heterogeneities in the entire rock cylinder, but more computing power and time will be needed to interpret the data.

In our 1D approach, a Kozeny-Carman correlation to derive permeability from porosity was used. Even if not presented here, this approach alone (no multiple local Pc curves) was not able to reproduce the amplitude of saturation profiles, confirming the statements made by Pairoys *et al.* [1]. To reproduce the amplitude of saturation profiles, we showed that it is required to introduce multiple local Pc curves. For this purpose, we used the Egermann approach that derives the local Pc from the calculation of the pressure profiles from the homogeneous interpretation. As said earlier, the Kozeny-Carman correlation was used to derive the permeability profile: this choice was driven by Pairoys *et al.* [1] results. Other models such as Timur [7] lead to too high permeability amplitudes. In our study, the Swanson MICP permeability values helped in validating the Kozeny-Carman method as best proxy, based on resulting permeability amplitudes. But other methods may be preferred if the MICP permeability amplitude variations were higher for instance.

In this study, we obtained different relative permeability curves using homogeneous and heterogeneous approaches. It differs from Pairoys *et al.* [1] observations. But what could be the reason(s)? It may be related to the degree of heterogeneity of the tested sample that looks more heterogeneous than that from Pairoys *et al.* [1] study: the CT image in Figure 1 highlights significant changes in texture at the centimetric scale, which was not the case when looking at the CT images acquired by [1] (Figure 32).

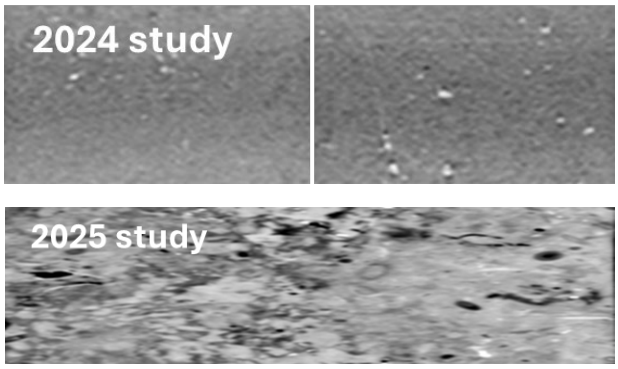

Fig. 32. Differences in CT images (2024 images at the top from reference [1], and 2025 image at the bottom from the current study).

Moreover, our current study highlights some longitudinal dispersion: even if MTT was not performed in [1], dispersive behavior would have been less pronounced based on the 2024 CT images.

Another interesting observation is the significant variation of local Pc curves: it provides an interesting Pc envelope that could be useful for constraining simulations at both core and reservoir scale. Additional simulations could be performed using the least oil-wet and most oil-wet Pc curves to provide a Kr envelope, with optimistic and pessimistic cases: it enables our lab to offer recommendations to reservoir engineers, helping them narrow the tuning range of Kr and Pc parameters when attempting to history-match reservoir production.

8 Conclusions

The main objective of the paper was to confirm, or not, the universality of the findings from the Pairoys *et al.* [1] study: improvement of the saturation profiles history-match quality and relative permeability Kr curves identical whatever the tested approach. i.e. homogeneous or heterogeneous approach.

To confirm the previous findings, a long core presenting a large degree of heterogeneity was selected. A water-oil steady-state Kr test was then performed at reservoir conditions, using 1D linear x-ray measurements of porosity and saturation profiles obtained at equilibrium during the test. The interpretation of the experimental results using Cydar software was first done by considering the rock as homogeneous. Then, we used the Egermann method with determination of the local capillary pressure curves at the 30 points of the x-ray in-situ measurements. This interpretation led to a fit of the experimental data (effluent and pressures) as good as those obtained with the homogeneous method but reproduced the noisy saturation profiles with good accuracy. This point is an improvement for the quality control of the simulation.

In this new study, and unlike the observation made by [1], the relative permeabilities determined with the heterogenous approach were found to be different from those considering the rock as homogeneous. Even if this result cannot be generalized, we highly recommend using this method especially after observing large degrees of heterogeneity via CT images, MICP and MTT. Other studies have shown similar observations: further work is necessary to explain the main reasons of the Kr difference using the two methods.

It is recognized that production scenarios in reservoirs are seldom accurately replicated using Kr values directly obtained from laboratory measurements due to various factors such as scale differences, presence of fractures, dynamic effects during production, and reservoir heterogeneity. Conducting representative lab waterflooding tests under reservoir conditions with reservoir fluids and using the heterogeneous approach can help mitigate discrepancies between field and laboratory observations. While further research is necessary to elucidate the reasons behind the differences observed between the 1D homogeneous and heterogeneous approaches, exploring 2D or even 3D heterogeneous approaches using advanced imaging techniques may provide deeper insight into the impact of small-scale heterogeneities during the coreflooding experiments.

Acknowledgements

The authors would like to thank SLB, Cydarex and TotalEnergies for permission to publish this work.

References

1. Pairoys, F., Lenormand, G., Lenormand, R.: “Determination of Relative Permeabilities on Heterogeneous Samples”, SCA2024-1077, 2024
2. Lombard, J.M., Egermann, P., Lenormand, R., Bekri, S., Hajizadeh, M., Hafez, H., Modavi, A., Kalam, M.Z.: “Heterogeneity Study through Representative Capillary Pressure Measurements – Impact on Reservoir Simulation and Field Predictions”, SCA2004-32, 2004
3. Egermann, P., Lenormand, R.: “A New Methodology to Evaluate the Impact of Localized Heterogeneity on Petrophysical Parameters (Kr, Pc) Applied to Carbonate Rocks”, Petrophysics, **46**, p. 335-345, 2005
4. Kozeny, J.: “Ueber Kapillare Leitung des Wasser sim Boden”, Sitzungsber Akad. Wiss., 1927
5. Carman, P.C.: “Fluid Flow through Granular Beds”, Transactions, Institution of Chemical Engineers, 1937
6. Pairoys, F., Caubit, C., Alexander, M., Ramos, J.: “Comparing Centrifuge, Steady-State and Semi-Dynamic Methods for Relative Permeability and Capillary Pressure Determination: New Insights”, SCA2021-019, 2021
7. Timur, A.: “An Investigation of Permeability, Porosity and Residual Water Saturation Relationship for Sandstone Reservoirs”, The Log Analyst, 1968